Full Paper

Berberis Aristata: A Highly Efficient and Thermally Stable Green Corrosion Inhibitor for Mild Steel in Acidic Medium

Nabin Karki,[1,2] **Shova Neupane,**[1,*] **Yogesh Chaudhary,**[1] **Dipak Kumar Gupta,**[1,3] **and Amar Prasad Yadav**[1,*]

[1]*Central Department of Chemistry, Tribhuvan University, Kathmandu, Nepal*
[2]*Bhaktapur Multiple Campus, Tribhuvan University, Bhaktapur, Nepal*
[3]*Trichandra Multiple Campus, Tribhuvan University, Kathmandu, Nepal*

*Corresponding Author, Tel.: +9779851124444

E-Mail: amar2y@yahoo.com

Abstract- Plant extracts are extensively researched as a source of green corrosion inhibitors. Herein, we report on a highly efficient and thermally stable corrosion inhibitor from the stem extract of high-altitude shrub *Berberis aristata*. The corrosion inhibition efficiency (*IE*) of the extract was tested in 1.0 M H_2SO_4 for the corrosion protection of mild steel (MS) by using gravimetric and electrochemical measurements. It displayed a remarkable *IE* of 90% at 200 ppm and reached to 98.18% at high concentration (1000 ppm) at room temperature. The thermal stability of the adsorbed extract was uncommon among the recently reported plant extracts, giving an *IE* of 80% at 338K. Besides, the adsorption of the extract was extremely efficient, producing an *IE* of 90% in 15 min. The thermodynamic parameters (ΔG and *Ea*) showed a chemisorption dominated behavior of the extract. Electrochemical measurements indicated a mixed type of inhibitor, and the extract suppressed the corrosion rate by blocking the active surface of the MS.

1. INTRODUCTION

The study of corrosion of mild steel (MS) is vital for academics and industrialists since it is an excellent material in a wide range of industries and machinery due to its mechanical properties, ease of fabrication, weldability, availability, and low cost. However, corrosion of MS is a major concern, and there have been tremendous efforts in minimizing the corrosion loss by adopting various strategies depending on the application areas [1]. Various acidic compositions are used to remove corrosion products, scales, or chalky deposits from the MS surface [2–5]. However, the used acidic medium also attacks the bare MS surface resulting in a reduction in materials strength. The effective remedy for this problem is the use of inhibitors. A recent trend of inhibitor is to explore environmentally friendly, non-toxic, and renewal component of plant sources [4, 6–8]. Plant sources contain large size organic molecules having active centers containing heteroatoms like N, S, O, and P in conjugation with multiple bonds or aromatic rings [9]. Such electron-releasing centers do a strong interaction with the MS surface to protect from aggressive corrosion medium.

Alkaloids containing phytochemicals present in plant extract are mainly responsible for corrosion inhibitive action. The common ways to characterize the inhibitive behavior of the plant extracts are to make weight loss and electrochemical polarization measurements [3, 7, 8, 10]. The effects of parameters like concentration of inhibitor, adsorption time, and temperature are found to be the prime focus of most studies.

In the recent past, plenty of plant sources have been studied as corrosion inhibitors for MS corrosion in acidic medium, and the inhibitive ability of their extracts have been found to be satisfactory to excellent [4, 6–26]. However, a primary concern for such inhibitors is their thermal stability, in most cases, desorption of the inhibitor molecules occurs at around 45°C (318 K), and inhibition efficiency drops below 40% [4, 8, 12]. As a matter of fact, this limits the applicability of the plant extracts at elevated temperature, which is necessary to remove the oxide layer or scale at shorter immersion time, and therefore, it requires a slightly elevated temperature, such as 50-60°C [5]. The thermodynamic calculations have shown that most of the plant extracts act as inhibitors due to mixed adsorption on metal surface involving both physical and chemical adsorption [8–10, 13–15]. Formation of coordinate covalent bond is attributed to the transfer of lone pair of electrons of heteroatoms or π electrons present in inhibitor molecules to vacant d-orbital of metal. The pairing efficiency of the molecule present in the plant extract as corrosion inhibitors depends upon the stability of formed chelate, corrosion medium, and possible steric effects [2, 4, 27].

In this study, we report the corrosion inhibition efficiency (*IE*) of high altitude (altitude: 1511 m) plant *Berberis aristata* of Nepalese origin. Nepal is rich in high altitude endemic plants, and many of them have been investigated as corrosion inhibitors for MS in acidic medium [28–33]. *Berberis aristata* is widely distributed from the northern Himalayan region to Sri Lanka, Bhutan, and hilly areas of Nepal. The main chemical constituent of this plant is

berberine. Berberine extracted from *coptis chinesis* has been reported as an effective inhibitor for MS and galvanized steels in acidic medium with temperature stability up to 45ºC [34, 35].

Similarly, berberine in *Mahonia neplensis* was found as mostly responsible for producing excellent inhibition efficiency for MS in acidic medium [36]. This research also showed the *IE* dominated by chemical adsorption and thermal stability up to 55°C. The stem extract of *Berberis aristata* chosen in this study is never tested for corrosion inhibition purpose to date. Therefore, the methanolic extract of *Berberis aristata* was evaluated as a highly efficient, thermally stable, and eco-friendly corrosion inhibitor for MS in acidic medium by electrochemical and gravimetric methods. The prime focus of this research was to analyze the effect of temperature, plant extract concentration, and adsorption time. Electrochemical evidences were complimented by estimating thermodynamic parameters of adsorption.

2. EXPERIMENTAL

2.1. Solution and specimen preparation

The stem of *Berberis aristata*, collected from Sipadol (latitude: 27º38'6.2" N, longitude: 85º25'58.7" E and altitude: 1511 m), Nepal were washed with distilled water, cut into smaller pieces and dried in the shade for one month. It was ground into a fine powder, dipped in methanol, shaken occasionally, and macerated for 72 hours at room temperature. After that, the supernatant liquid was collected by repeated filtration until a clear supernatant liquid, which was concentrated using IKA RV-10 digital rotary evaporator. The suspension was further dried using a water bath to obtain a solid residue, which is *Berberis aristata* extract (BAE). 1.0 g of BAE was dissolved in 1000 mL of warm 1.0 M H_2SO_4 to prepare a stock solution (1000 ppm), and the undissolved residue was discarded by filtration. The stock solution was further diluted with 1.0 M H_2SO_4 to prepare 800, 600, 400, and 200 ppm solutions.

A flat sheet of commercial mild steel (MS) available in the local market of Nepal was used in this study. The MS sample of dimensions of 3.25 cm×3.25 cm×0.15 cm and 2 cm×2 cm×0.15 cm were used for gravimetric and electrochemical experiments, respectively. Each sample was mechanically polished with silicon carbide (SiC) paper till #1200 grit size. The abraded samples were cleaned ultrasonically with anhydrous ethanol for 15 min to remove residual particles, dried with air blower, and stored in a desiccator.

2.2. Characterization of extract and metal surface

A Fourier transform infrared (FTIR) spectrum in attenuated total reflectance (ATR) mode of the BAE was recorded using a Shimadzu FTIR spectrophotometer. The obtained spectra were analyzed to ensure the presence of different functional groups in the BAE extract. A Bio-Logic M470 Ac-SECM scanning electron microscope (SEM) in conjugation with an energy dispersive X-ray (EDX) was used to observe the morphological changes of MS surface

immersed in 1.0 M H_2SO_4 and 1.0 M H_2SO_4+ BAE for 24 h. The surface analyses of the MS sample were performed at three different locations to ensure reproducibility. Similarly, EDX analysis was carried out employing a beam of accelerating voltage of 15 KV for elemental analysis.

2.3. Electrochemical measurements

Electrochemical measurements involved open circuit potential (OCP), potentiodynamic polarization and electrochemical impedance spectroscopy (EIS) measurements in different concentrations of BAE. A gamry reference 600 potentiostat was used to perform these measurements. A three-electrode cylindrical glass cell with a saturated calomel electrode (SCE) as a reference electrode and a platinum wire as a counter electrode were used. The potential value mentioned hereafter is referred to as SCE. OCP was measured for 20 min to let the MS sample attain a steady-state condition before running potentiodynamic polarization. The polarization was started from a cathodic potential limit of -0.30 V vs. OCP to anodic limit of +0.30 V vs. OCP at a scan rate of 0.5 mV/s. Corrosion potential (E_{corr}), corrosion current (I_{corr}), and Tafel slopes were estimated to evaluate the *IE* of the BAE on MS corrosion in 1.0 M H_2SO_4 with the following equation (1) [10],

$$IE\% = \left(1 - \frac{I_{corr}}{I_{corr}^0}\right) \times 100\%$$
(1)

where corrosion current densities with and without inhibitor are I_{corr} and I_{corr}^0, respectively.

For *EIS* measurements, a sinusoidal voltage of 10 mV peak to peak at frequencies between 100 kHz to 0.01 Hz was applied at OCP. A simple Randles circuit consisting of a single time constant was used to fit the data. The R_{ct} value thus obtained was used to estimate the *IE* by the equation (2) [10],

$$IE\% = \left(1 - \frac{R_{ct}^0}{R_{ct}}\right) \times 100\%$$
(2)

where charge transfer resistances with and without inhibitor are R_{ct} and R_{ct}^0, respectively.

2.4. Gravimetric measurements

Gravimetric analyses were carried out with triplicates samples to study the effect of time, concentration, and temperature. Weight of the clean MS sample was taken before and after corrosion in 1.0 M H_2SO_4 solution containing different amounts of BAE. The sample was thoroughly rinsed in the running distilled water after each immersion measurements, dried with compressed air, and preserved in a desiccator. An Ohaus E1RR80 analytical balance was used to take the weight of samples before and after immersion. The measurement temperature was varied from 298 to 338 at 10 K interval, and the temperature-control was achieved by a Clifton water bath (NE2-4D). From the temperature effect, the thermodynamic parameters and

adsorption isotherms were calculated. The concentration of BAE solution used were 1000, 800, 600, 400, and 200 ppm. The effect of time on corrosion inhibition efficiency of BAE was estimated at 1000 ppm of BAE.

The equation (3) was used to calculate the corrosion rate (*CR*) of MS sample in each set of experiment [10]:

$$CR = \frac{87.6W}{AtD} \tag{3}$$

where *W* is weight loss (mg), *A* is the surface area (cm^2), *t* = time of immersion (h) and *D* is the density of the MS sample (g/cm^3)

The inhibition efficiency (*IE*) and surface coverage (*θ*) were calculated by equations (4) and (5), respectively [10]:

$$IE\% = \left(1 - \frac{CR_2}{CR_1}\right) \times 100 \tag{4}$$

where, CR_1 and CR_2 are the corrosion rates in the absence and presence of inhibitor, respectively.

$$\theta = \left(1 - \frac{W_2}{W_1}\right) \tag{5}$$

Where, W_1 and W_2 are the weight loss in the absence and presence of inhibitor, respectively.

3. RESULTS AND DISCUSSION

3.1. ATR-FTIR analysis

Fig. 1a shows the ATR-FTIR spectra of the BAE extract with representative functional groups. Broadband in the range of 3360 cm^{-1} to 3209 cm^{-1} is attributed to O-H stretching of alcohol, phenol, carbohydrate, and N-H stretching of amine. A band at 2912 cm^{-1} is due to C-H stretching of alkane while the band at 1650 cm^{-1} represents C=C stretching, C=N stretching of imine or oxime, C=O stretching of amide or δ-lactum and N-H bending of amine. A sharp band at 1570 cm^{-1} is associated with aromatic C=C bending and N-H bending of amine. Similarly, the absorption band at 1435 cm^{-1} is due to O-H bending of carboxylic acid, and a sharp peak at 1384 cm^{-1} is for O-H bending of alcohol, phenol, and C-H bending of gem dimethyl or aldehyde. A band at 1284 cm^{-1} is ascribed to C-N stretching of aromatic amine which is further supported by a sharp peak at 1037 cm^{-1}. The absorption band at 1200 cm^{-1} is attributed to C-O stretching of aromatic ether, 3° alcohol, ester, C-N stretching of amine, and band at 1103 cm^{-1} is related to C-O stretching of 2 ° alcohols, ether, C-N stretching of amine. There is again a band at 987 cm^{-1} due to C=C bending of the alkene. These absorptions bands divulge that extract contains functionalities like alcohol, phenol, amine, ether, carboxylic acid,

carbohydrate with aromatic rings. Aromatic rings with heteroatoms like N, O make the BAE extract as a promising candidate for corrosion inhibitor of MS[16]. The major compounds in the methanolic extract of Berberis aristata are Berberine, Jatrorrhizine, 7,8-dihydro-8-hydroxy berberine, Berbamine, Oxyberberine, Pakistanamine, as shown in Fig. 1b[37–39].
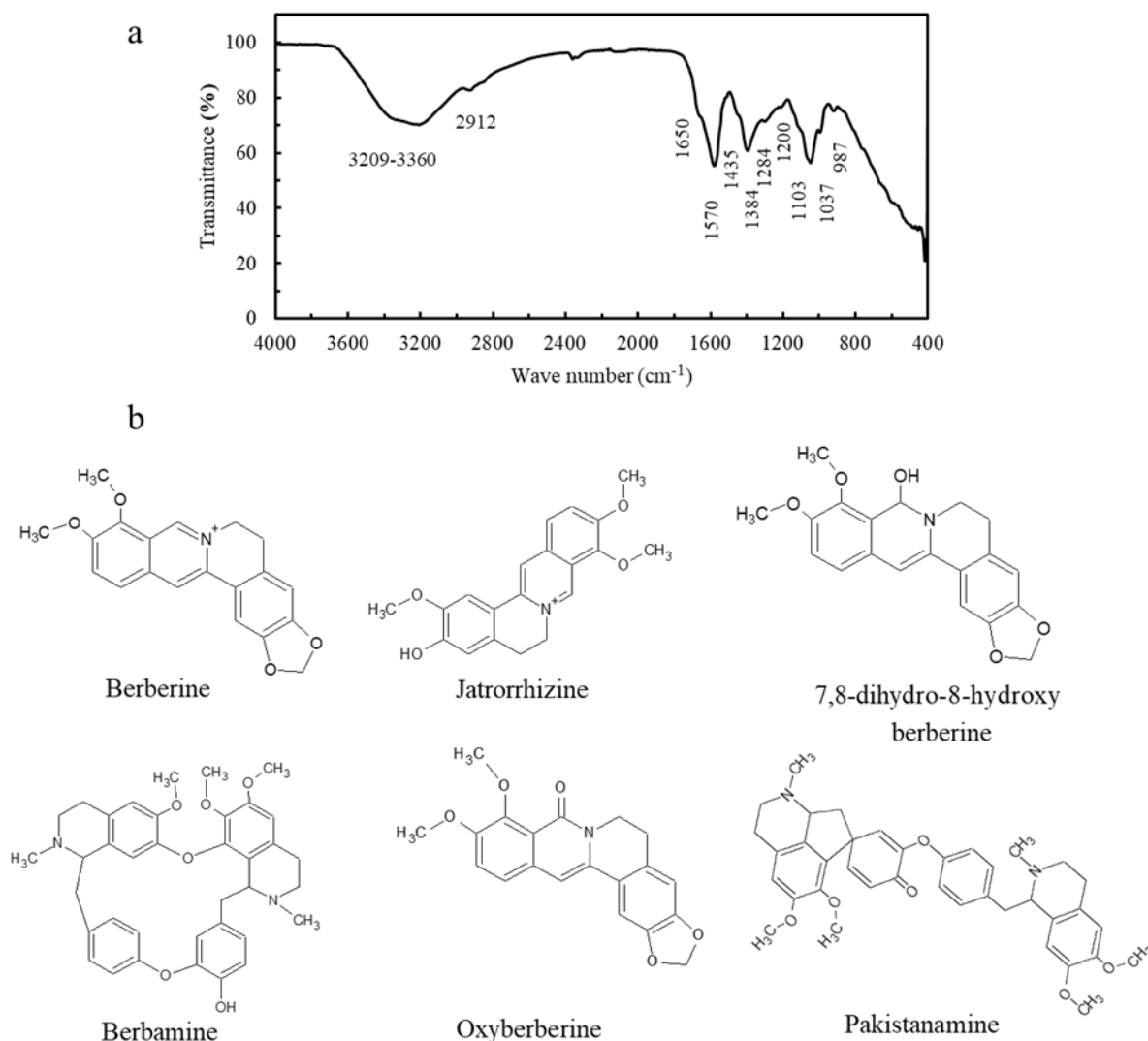

Fig. 1. a) FTIR spectra of the extract of *Berberis aristata*, b) Structure of a few compounds isolated from methanol extract of *Berberis aristata*

3.2. Electrochemical measurements

Fig. 2a shows the variation of OCP of MS in 1.0 M H_2SO_4 containing different amounts of BAE. There is a negligible change of OCP with BAE solution as compared to 1.0 M H_2SO_4 solution. This phenomenon shows that the BAE acts as a mixed type of inhibitor [17]. The marginal shift of OCP towards positive value is due to the adsorption of molecules present in BAE.
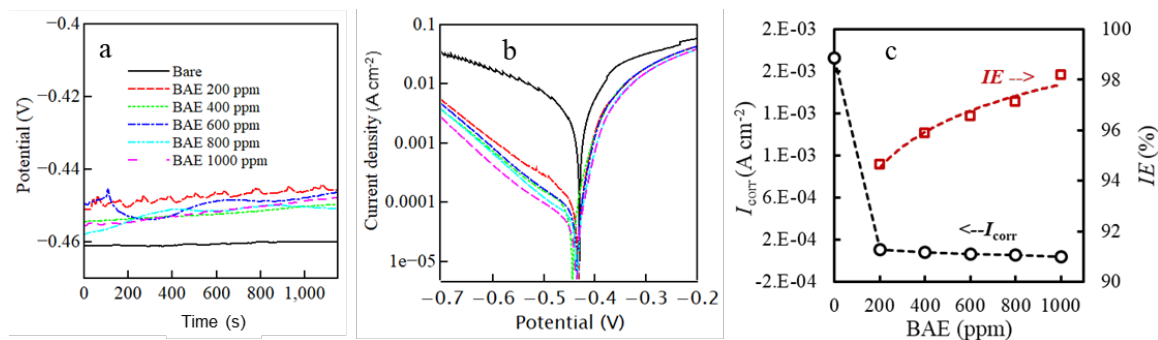
Fig. 2. a) Variation of OCP b) Polarization curve of MS sample in 1.0 M H₂SO₄ with different concentrations of BAE. c) the variation of Icorr and IE with the concentration of BAE

The potentiodynamic polarization curves presented in Fig. 2b shows a significant suppression of cathodic current with the addition of BAE. The cathodic and anodic Tafel slopes remain in the range of 0.114 V/decade and 0.028 V/decade, respectively. These values are typical for hydrogen evolution and Fe-dissolution reactions [40].

Fig. 2c shows the variation of I_{corr} with the concentration of BAE and corresponding *IE*. It can be seen that a 1000 ppm BAE solution lowered the I_{corr} value by 55 times, enlisting an *IE* of 98.18%. The lowest concentration of the BAE, 200 ppm, also significantly suppressed the I_{corr} by about 19 times and producing an *IE* of approximately 95%, which is an excellent efficiency shown by a lower concentration of the extract [9, 18, 19]. These values of *IE* indicate that BAE by adsorbing effectively on the MS surface acts as an excellent inhibitor for corrosion protection of MS in acidic medium. Adsorption might be enhanced due to the synergistic effect of different organic compounds present in the BAE, which will be discussed further in a later section.

EIS was also used to study the effect of BAE on steady-state corrosion behavior of MS in 1.0 M H₂SO₄ at OCP in a wide range of frequencies. Fig. 3a and 3b show the Nyquist and Bode phase plots at various concentrations of BAE. The symbols represent the measured data, and solid lines represent the fitting data using Z-View (3.1c version) software using a simple equivalent circuit, as shown in Fig. 3c.

A similar shape of EIS plots in the presence of BAE inhibitor of different concentrations implies a single relaxation process with similar corrosion mechanisms as the bare counterparts. High-frequency dispersion in the capacitive loop is typical of solid electrodes following surface roughness [41]. Furthermore, non-homogeneity of structural or interfacial origin prevalent in the adsorption processes also contributes to high-frequency dispersion [41]. The presence of inductive loop at low-frequency region, whose diameter increases with the concentration of BAE, is indicative of the relaxation process associated with adsorption-desorption of inhibitor molecules on the electrode surface accompanied by re-dissolution of the inhibited surface. It may be due to the consequence of the layer stabilization by intermediate products on electrode surface such as $[FeSO_4^{-2}]_{ads,}[FeOH]^-_{ads}$, $[FeH]^+_{ads}$ involving inhibitor molecules. The effect of

adsorption of inhibitor molecules of BAE on MS surface is reflected in the Bode-phase plot. The adsorption of BAE has significantly increased the phase angle.
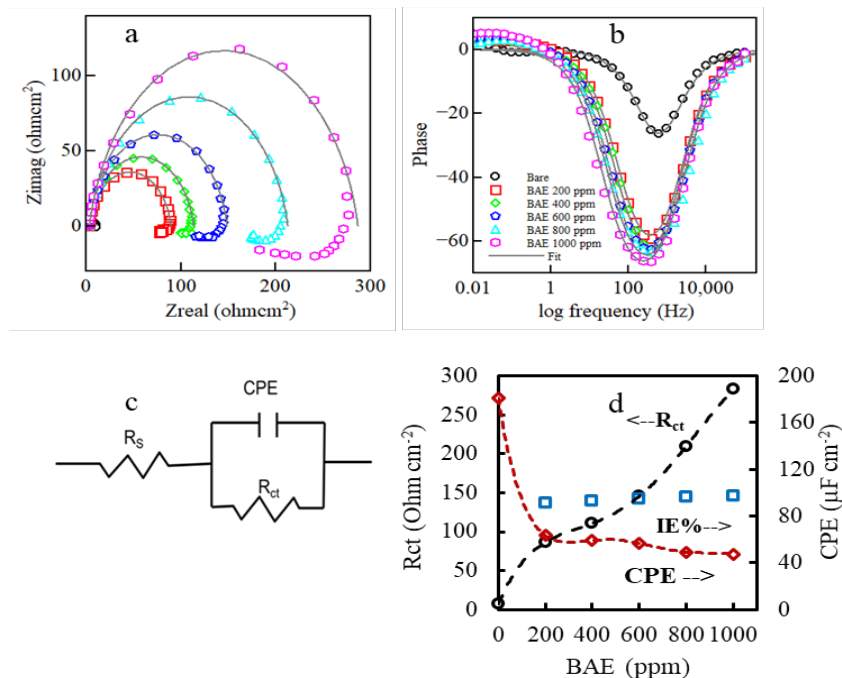

Fig. 3. a) Nyquist plots b) Bode phase plots of phase angle vs. frequency for MS in 1.0 M H_2SO_4 with BAE of different concentrations c) The equivalent circuit model used to fit the impedance spectra. d) The change of R_{ct}, C_{dl} and IE with concentration

Fig. 3d shows the variation of R_{ct} and CPE values estimated from fitting the Nyquist plot in Fig. 3a. There is a gradual increase of R_{ct} with the concentration of BAE due to more considerable surface coverage as more inhibitor molecules are available. Oppositely, the CPE value drastically decreased with the addition of BAE and almost remains constant at higher concentrations. The decrease of CPE with BAE is attributed to decrease in the local dielectric constant of the double-layer with an increase in the thickness of the electric double layer. This might be due to the large size of the inhibitor molecule, which gradually replaces water molecules. The IE estimated from the R_{ct} values is also depicted in Fig. 3d, which shows values above 92% at 200 ppm to 98% at 1000 ppm. This again indicates that the BAE acts as a promising inhibitor for the corrosion protection of MS in acidic medium.

3.3. Gravimetric Measurement

Gravimetry was used to study the effect of long time immersion of MS samples in BAE acidic solutions. Fig. 4a shows the results of gravimetric measurements in 1000 ppm BAE solution for 0.25 h, 0.75 h, 1.5 h, 3 h, 6 h, 9 h, 12 h, and 24 h at 298 K and the corresponding *IE* calculated from the obtained results. The plot implies that the corrosion of MS is significantly inhibited by the addition of BAE as an inhibitor, and inhibition increases with

time, reaching a value of approximately 97.0% after 24 h of immersion in 1.0 M H_2SO_4 solution. The result is clear evidence that BAE is effective and efficient inhibitor acting promptly by adsorbing on MS surface, thereby producing an *IE* of above 90% in just 0.25 h after immersion in acidic solution. Such a fast inhibition of corrosion is essential for practical applications of the inhibitor[5].
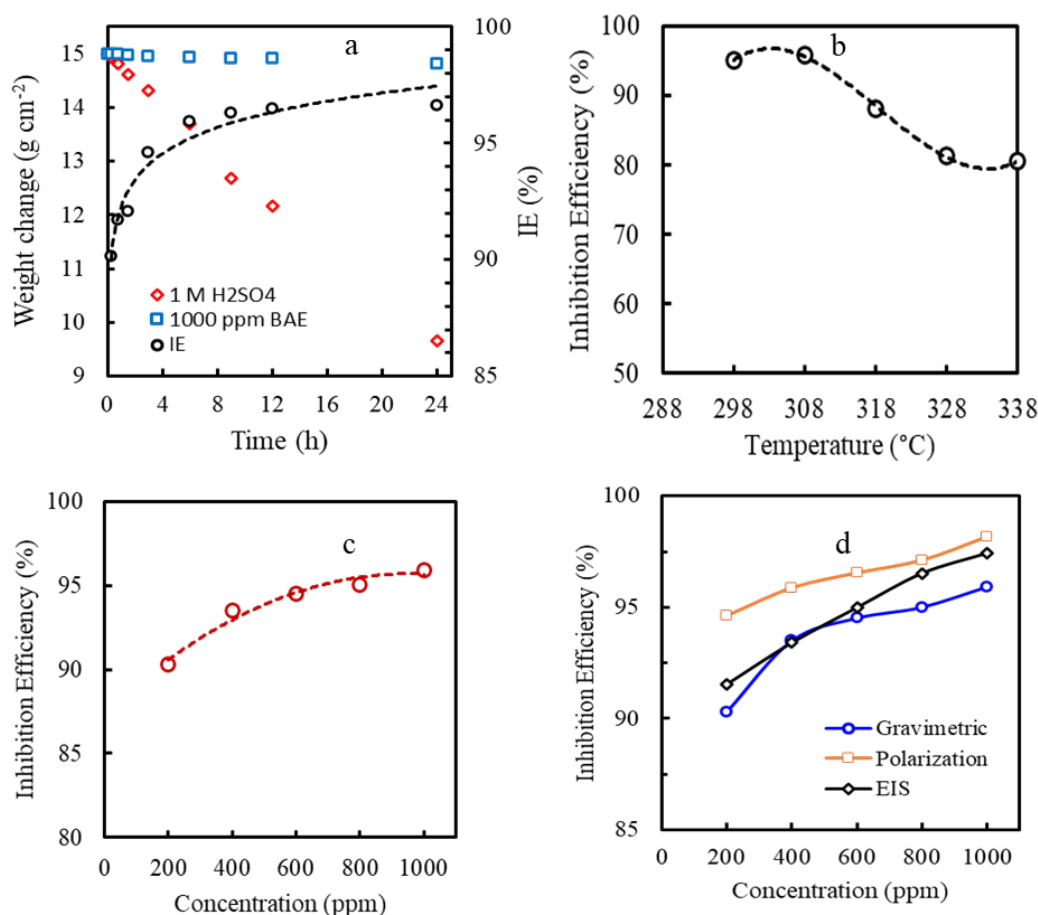

Fig. 4. a) Variation in weight of MS sample immersed in the presence and absence of BAE together with the variation of *IE* with immersion times. Variation of inhibition efficiency of BAE on mild steel surface at b) different temperatures, c) different concentrations and d) from different methods

The stability of barrier film formed due to adsorption of inhibitor on MS surface as well as activation parameters of the corrosion process of MS in acidic media was studied by gravimetric at various temperatures (298 K, 308 K, 318 K, 328 K, 338 K) for 6 h in 1000 ppm BAE solution. The effect of temperature on the corrosion rate and inhibition efficiency is shown in table 1 and represented in Fig. 4b. The *IE* remains the same till 308 K, and after that decreases marginally and stays constant at 80% after 12 h. This result is very encouraging for plant extracts as a corrosion inhibitor as in most cases the *IE* has been reported to fall below

40% at such temperature [4, 11, 12]. Such a higher *IE* at 338 K (65 ˚C) can be beneficial for other applications as well, such as for removing corrosion products for weight loss estimation [5]. Similarly, this will allow for faster removal of scales and oxide layers in the industrial process used for surface finish. Berberine extracted from *Coptis chinesis,* though showed similar *IE* to this study, but temperature stability was not like BAE [34, 35]. Therefore, isolation of the various components of BAE should be done to understand the higher temperature stability of the extract of *Berberis aristata*. The study should clarify the desorption characteristics of various components of BAE at higher temperatures.

Table 1: Corrosion rate of mild steel and inhibition efficiency of BAE for mild steel corrosion at various temperatures.
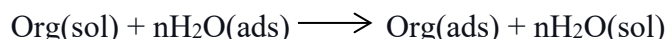
Temperature (K)	Corrosion Rate (mg/cm^{2}h)		Inhibition Efficiency (*IE*) (%)
	Only acid	Acid with inhibitor	
298	74.87	3.65	95.13
308	129.21	5.27	95.92
318	199.99	23.75	88.12
328	273.77	50.94	81.39
338	386.51	75.27	80.53

The effect of BAE concentrations on *IE* is shown in Fig. 4c. The MS sample was immersed in several BAE solutions for 6 h at 298 K. The effectiveness of the BAE can be seen from the figure, where 200 ppm of the extract is enough to inhibit with the corrosion of MS by 90.32%, and maximum *IE* reaches a value of 96.0% at 1000 ppm. There are not many plant extracts giving in *IE* of 90% at 200 ppm [9, 18, 19]. An increase in *IE* with the concentration of extract can be ascribed to the more surface coverage of MS by the extract molecules. The result is in agreement with electrochemical tests such as potentiodynamic polarization and EIS. A comparison of inhibition efficiency obtained by different methods is shown in Fig. 4d, showing similar *IE* by all the methods.

3.4. Adsorption isotherm

Adsorption isotherm of BAE on MS is necessary to understand the interaction degree between inhibitor molecules and MS surface. A spontaneous adsorption of inhibitor molecules is feasible if the interaction energy between the molecules and the MS surface is higher than that of water molecules and MS surface. Adsorption depends upon chemical composition, the molecular structure of inhibitor, temperature, and the electrochemical potential at the metal/solution interface. In the process, the solvent water molecules could also adsorb-desorb at the metal/solution interface. So, this adsorption can be considered as a quasi-substitution

process between the inhibitor molecules in aqueous phase [org(sol)] and water molecules at the electrode surface [H_2O(ads)]:

$$Org(sol) + nH_2O(ads) \longrightarrow Org(ads) + nH_2O(sol)$$

where, n is the number of water molecules replaced by one inhibitor molecule.

The degree of surface coverage (θ) obtained by the gravimetric method was plotted as a function of inhibitor concentration to evaluate the best isotherm that fits the data obtained in the present study. As for the inhibitor concentration used for fitting the suitable adsorption model, an average molar concentration of few important compounds listed in Fig. 1(b), which plays a vital role in inhibition, is used [8]. Several adsorption isotherms, such as Langmuir, Tempking, Freundlich, El-Awady, were tested to describe the adsorption behavior of inhibitor, in which best fit was obtained in Langmuir adsorption isotherm. A plot of C_{inh} against C_{inh}/θ in Fig. 5 shows a straight line with values of linear correlation coefficient (R^2) and slope equal to about 1. Little deviation of slope from unity can be attributed to some interactions between adsorbed molecules on MS surface, which may be mutual attraction or repulsion between different functional groups of molecules or preferential adsorption of molecules at the cathodic and anodic site[17,41]. According to Langmuir's assumption, adsorption of inhibitor molecules on MS surface in the present study leads to monolayer formation where adsorbate molecules do not interact with each other.
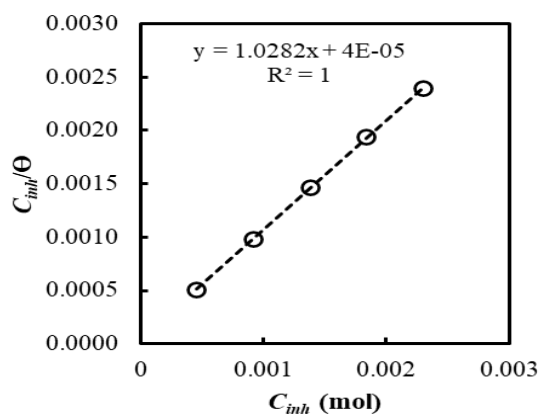

y = 1.0282x + 4E-05
$R^2 = 1$

Fig. 5. Langmuir adsorption isotherm plot for mild steel in 1.0 M H_2SO_4 with different concentrations of BAE as the average molar concentration of some major compounds in BAE

Adsorption isotherm given by Langmuir is given in equation (6) [4].

$$\frac{C_{inh}}{\theta} = \frac{1}{K_{ads}} + C_{inh} \qquad (6)$$

Value of adsorption constant (K_{ads}) can be obtained from the slope of Langmuir adsorption isotherm plot in Fig. 5 and this value can be used to compute the value of free energy of adsorption (ΔG^o) according to equation (7) [10]:

$$\Delta G^o = -RT \ln(55.5 K_{ads}) \tag{7}$$

where, R is the universal gas constant (8.314J/mol K), and 55.5 is the concentration of water in solution in mol/L. The calculated value of ΔG^o according to relation (7) is -35.05 KJ/mol. A significant negative value of ΔG_{ads}^o indicates that adsorption of BAE on MS surface is spontaneous with the formation of a highly stable adsorbed layer [10, 42]. Generally, the value of ΔG^o less than or around -20 KJ/mol is associated with physisorption, and more than or around -40 KJ/mol is associated with chemisorption. Since the calculated value ΔG^o is more than the intermediate value, it can be concluded that adsorption is mainly dominated by chemisorption [10, 42]. The adsorption of inhibitors molecules is due to the electrostatic interaction between charged BAE molecules and charged MS surface with replacement of water molecules from the MS surface. This is further followed by chemisorption with the formation of a coordinate type of bond due to charge transfer from organic molecule to vacant d-orbital of Fe [10].

3.5. Calculation of activation energy and thermodynamic parameters

Corrosion rate depends upon the temperature and temperature dependency is given by Arrhenius equation (8) [4]:

$$\log(CR) = \log A - \frac{E_a}{2.303\,RT} \tag{8}$$

where E_a is the activation energy, A is the Arrhenius pre-exponential constant, T is the absolute temperature. From the Arrhenius plot in Fig. 6a, the value of E_a is calculated and tabulated in table 2. A significant increase in E_a with the addition of BAE reflects a strong adsorption of inhibitor molecules on the metal surface [20]. The literature values of some of the plant extracts show the E_a value in the range of 40 KJ/mol [8, 10, 14, 20, 21]. Therefore, it can be plausibly assumed that higher thermal stability of BAE is due to the higher energy of activation of molecules in BAE. However, as mentioned above, it is necessary to isolate the various compounds in BAE and check the *IE* of individual molecules so that higher thermal stability of BAE can be explained.
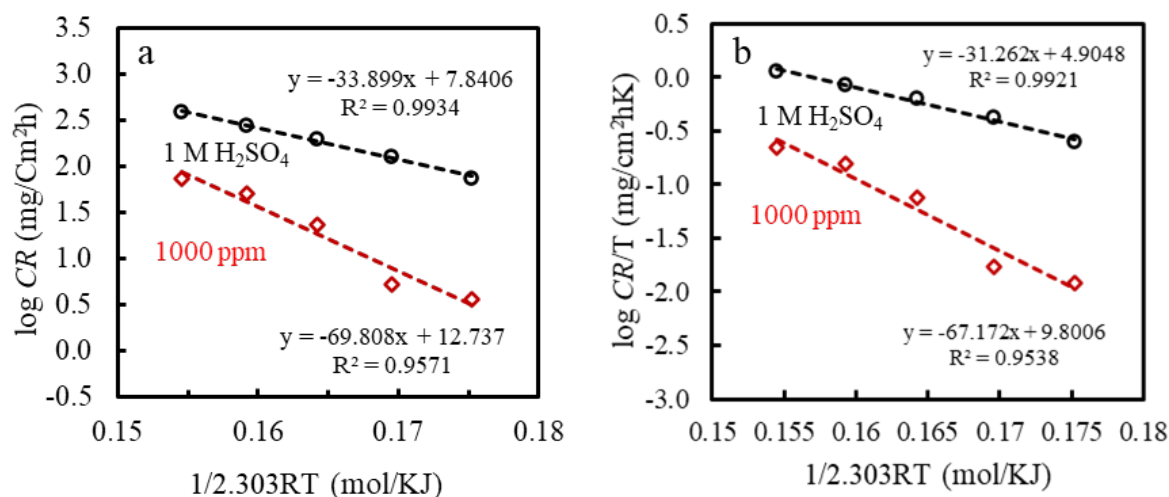
Fig. 6. a) Arrhenius plot for mild steel in 1.0 M H₂SO₄ with and without BAE, b) Transition state plot for mild steel in 1.0 M H₂SO₄ with and without BAE

The change in entropy and enthalpy of the adsorption can be calculated from transition state equation (9), where the slope of line obtained by plotting log(CR/T) vs. 1/2.303RT is enthalpy and entropy can be calculated from intercept [4]:

$$\log\left(\frac{CR}{T}\right)=\left[\log\left(\frac{R}{hN}\right)+\left(\frac{\Delta S^{*}}{2.303R}\right)-\frac{\Delta H^{*}}{2.303\,RT}\right] \tag{9}$$
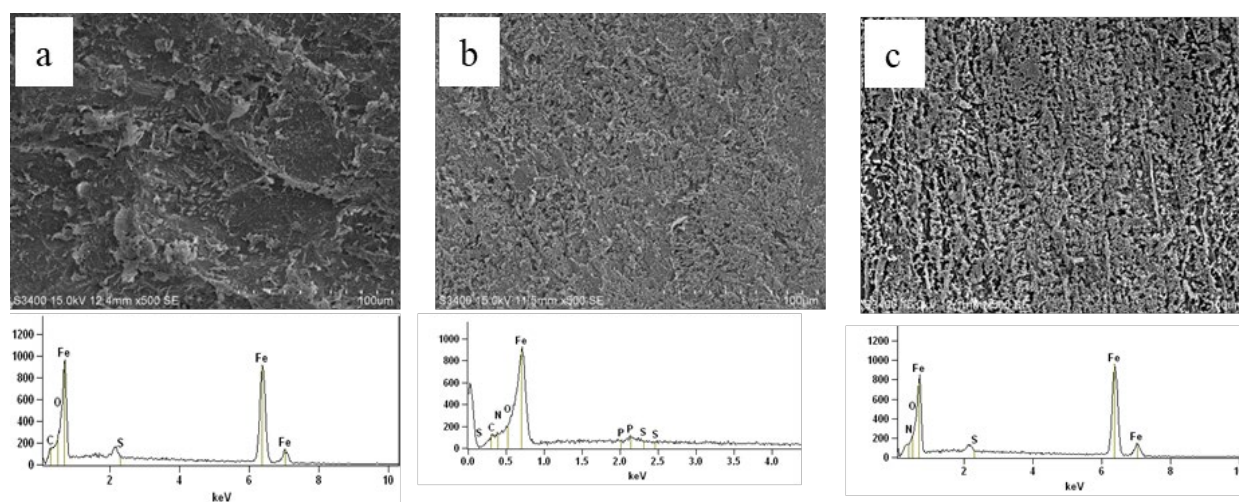
where h is plank's constant, 6.6261×10^{-34} Js and N is the Avogadro's number, 6.0225×10^{23} mol⁻¹.

The values of ΔH^* and ΔS^* for acid without and with inhibitor are compared in table 2. An intermediate value of ΔH^* (67.17 KJ/mol) reflects a mixed type of adsorption of BAE molecules involving physisorption and chemisorption[22]. In addition, the positive and relatively more tremendous value of ΔH^* implies the control of corrosion by the kinetic factors. Similarly, the higher value of Ea than that of ΔH^* indicates a decrease in the total reaction volume due to the involvement of a gaseous reaction, merely the hydrogen evolution reactions[4]. The difference in the value of Ea and ΔH^* is nearly equal to RT, which divulges that the corrosion process is unimolecular.

The shift of ΔS^* towards positive value by the addition of BAE indicates an increase in disorder of the system on going from reactant to activated complex. This behavior can be explained due to the replacement of water molecules during the BAE adsorption on the metal surface [20]. However, it is not common to get such a significant increase in ΔS^* value with the addition of plant extracts, and many plant extracts have shown a lower change in ΔS^* value [16, 23–25]. This again needs to be investigated further so that higher thermal stability of BAE can be understood and more such inhibitor molecules can be designed or isolated.

Table 2. Activation parameters of the dissolution of mild steel in 1.0 M H_2SO_4 in the presence of 1000 ppm concentration

Electrolyte	*Ea* (KJ/mol)	*ΔH* (KJ/mol)	*Ea-ΔH*	*ΔS* (J/molK)
1.0 M H_2SO_4	33.9	31.26	2.64	–103.66
Acid with inhibitor (1000 ppm)	69.81	67.17	2.64	–9.93

Fig. 7. SEM images and corresponding EDX spectra of mild steel coupons after 24 hrs immersion in (a) 1.0 M H_2SO_4 (b) 400 ppm extract solution in 1.0 M H_2SO_4 (c) 1000 ppm extract solution in 1.0 M H_2SO_4

3.6. Surface analysis

SEM and EDX measurements were carried out to observe the surface morphological changes and presence of heteroelements on the MS surface after 24 h immersion in the BAE solutions. Fig. 7 shows some severe surface damage with deep furrows, and large cracks on the sample immersed in acid. These cracks and furrows are not seen in the surface immersed in acid with BAE. It displays a relatively smooth surface with the formation of a protective film. EDX shows the amount of nitrogen increased on the BAE covered surface, which indicates the molecular presence of nitrogen containing species in BAE.

3.7. Mechanism of inhibition

The molecular adsorption on the MS surface depends on the surface charge, chemical structure, dipole moment of inhibitor molecules, and the role of additional ions. Extract of *Berberis aristata* contains large size aromatic organic molecules with heteroatoms; prominent among them are berberine family molecules. These molecules can be adsorbed on the metal surface and inhibit corrosion either by physical adsorption due to electrostatic force of attraction between the charged metal surface and inhibitor molecules or by chemical

adsorption due to the sharing of π-electrons or lone pair of electrons of heteroatoms. These features will be further supported by electron-releasing centers such as the methyl group. Thermodynamic parameters such as the free energy of adsorption (-35.05 KJ/mol) and energy of activation (69.81 KJ/mol) point to the chemisorption dominated behavior of BAE on the MS.

BAE contains berberine family molecules with quaternary nitrogen with a positive charge. In acidic medium, amino nitrogen, phenolic or ethereal oxygen gets protonated. So, inhibitor molecules will be positively charged. The OCP of MS in BAE is measured around -0.44 V, which is positive than the potential of zero charge (PZC) of MS in sulfate solution [43]. When the value of PZC is less than that of OCP, the value of Antropov's rational corrosion potential becomes positive, and the net charge on MS gets positive. In such conditions, there will be electrostatic repulsion between the protonated inhibitor molecule and the metal surface. However, sulfate ions derived from H_2SO_4 are adsorbed on the metal surface due to a small degree of hydration, which results in the excessive negative charge close to the interface and favors the adsorption of positively charged protonated inhibitor molecules. Thus, inhibitor molecules get adsorbed on the metal surface through the sulfate bridge. In other words, there is a synergism between sulfate ion and inhibitor molecules for physical adsorption. This adsorption of BAE molecules will compete with adsorption of H^+ ion on the cathodic site of MS leading to suppression of cathodic hydrogen evolution.

In addition to physisorption, neutral or cationic inhibitor molecules may be adsorbed by chemisorption as well with replacement of water from MS surface by inhibitor molecules. Chemisorption is due to the interaction of the highest occupied molecular orbital (HOMO) of organic molecules with vacant d-orbital of iron to form a coordinate bond (donor-acceptor interaction). HOMO is the orbital with larger electron density, such as bonding π-orbital or lone pair of electrons. Due to electron pair on heteroatoms, the large organic molecules in BAE acts as a soft base with large polarizability accompanied with low ionization potential. The bulk metal or metal at zero oxidation state behaves as a soft acid. According to Hard and Soft Acid and Base (HSAB) theory, soft acid reacts faster and forms a strong bond with a soft base. So, stronger donor-acceptor interaction is expected between electrons of the inhibitor to the metal atom [44]. This interaction results in the accumulation of extra negative charges on the metal surface. To relieve this extra charge, electrons may be given back from 4s or 3d orbital of the metal atom to lowest unoccupied molecular orbital (LUMO) of BAE molecules to form a feedback bond. LUMO is a vacant antibonding π* orbital of organic molecules with larger orbital density. The presence of two tertiary nitrogen centers together with electron- releasing methyl groups seems to be making the adsorption of BAE very useful.
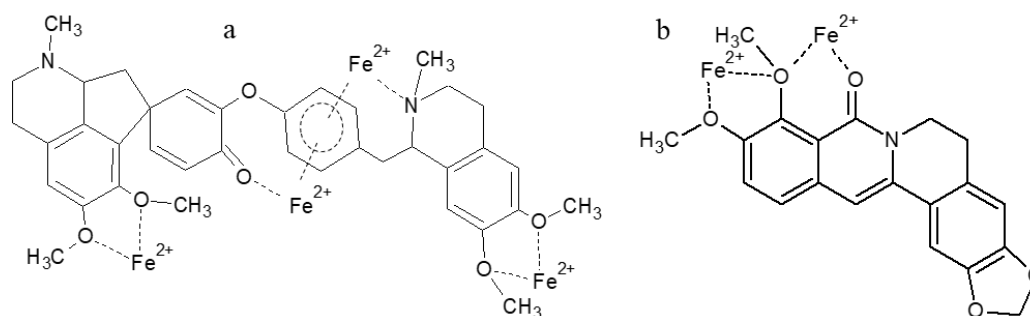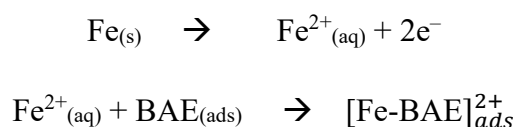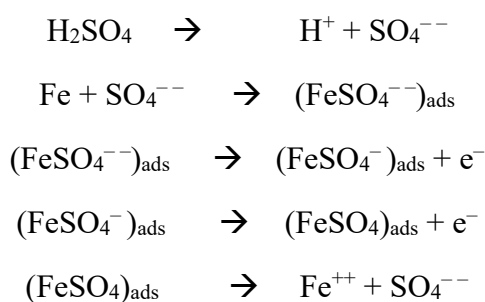
Fig. 8. Metal inhibitor chelate complex formed by iron with (a) Pakistanamine (b) Oxyberbeine

Besides, inhibition can also be explained by the chelation of Fe^{2+} with BAE molecules leading to the formation of a stable insoluble metal-inhibitor complex. After the formation of a number of such types of complex molecules, the solubility of the protective layer decreases, which suppresses the anodic metal dissolution and hence prevents the corrosion. It explains the increase in inhibition efficiency with the increase in concentration and time. The possible chelate complexes of two organic molecules are shown in Fig. 8.
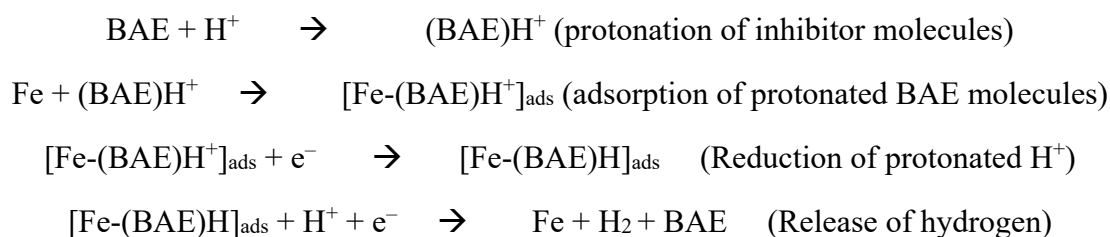
Chelation inhibits the anodic reaction as follows:

$$Fe_{(s)} \quad \rightarrow \quad Fe^{2+}_{(aq)} + 2e^-$$

$$Fe^{2+}_{(aq)} + BAE_{(ads)} \quad \rightarrow \quad [Fe\text{-}BAE]^{2+}_{ads}$$

The adsorption of inhibitor molecules inhibits both anodic and cathodic reactions. Anodic dissolution is suppressed by the adsorption of sulfate ions which is shown as follows [26]:

$$H_2SO_4 \quad \rightarrow \quad H^+ + SO_4^{--}$$

$$Fe + SO_4^{--} \quad \rightarrow \quad (FeSO_4^{--})_{ads}$$

$$(FeSO_4^{--})_{ads} \quad \rightarrow \quad (FeSO_4^-)_{ads} + e^-$$

$$(FeSO_4^-)_{ads} \quad \rightarrow \quad (FeSO_4)_{ads} + e^-$$

$$(FeSO_4)_{ads} \quad \rightarrow \quad Fe^{++} + SO_4^{--}$$

The cathodic hydrogen evolution is suppressed due to adsorption as:

$$BAE + H^+ \quad \rightarrow \quad (BAE)H^+ \text{ (protonation of inhibitor molecules)}$$

$$Fe + (BAE)H^+ \quad \rightarrow \quad [Fe\text{-}(BAE)H^+]_{ads} \text{ (adsorption of protonated BAE molecules)}$$

$$[Fe\text{-}(BAE)H^+]_{ads} + e^- \quad \rightarrow \quad [Fe\text{-}(BAE)H]_{ads} \quad \text{(Reduction of protonated } H^+)$$

$$[Fe\text{-}(BAE)H]_{ads} + H^+ + e^- \quad \rightarrow \quad Fe + H_2 + BAE \quad \text{(Release of hydrogen)}$$

4. CONCLUSION

The methanol extract of *Berberis aristata* is found to be an effective corrosion inhibitor for MS in 1.0 M H_2SO_4. Inhibition efficiency is above 90% at 200 ppm concentration of BAE. The *IE* increases with an increase in concentration, and maximum *IE* of 98.14% is obtained for 1000 ppm solution by potentiodynamic polarization. The thermal stability of the BAE on MS surface is exceptionally high, giving an *IE* of 80% at 338 K. The BAE is found to be a highly efficient inhibitor giving 90% efficiency in 0.25 h in 1000 ppm solution. The inhibition of corrosion of MS is due to monolayer adsorption of inhibitor molecules on the metal surface, and the adsorption follows the Langmuir adsorption isotherm. Values of ΔG^o and Ea indicate the adsorption of molecules on the MS is dominated by chemical adsorption.

Meanwhile, values of ΔH^* and Ea indicate that the adsorption process is unimolecular and endothermic. Electrochemical parameters show that it is a mixed type of inhibitor which significantly suppresses the cathodic reaction. EDX and SEM analysis confirm the formation of the surface film of BAE on the MS surface and inhibit the corrosion by barrier layer action.

Acknowledgments

Conflicts of interest: The author declares no conflicts of interest.

Supplementary material: The corresponding author provides supplementary material upon a reasonable request.

REFERENCES

[1]   E. E. Oguzie, Y. Li, and F. H. Wang, Electrochimica Acta 52 (2007) 6988.
[2]   M. Murmu, S. K. Saha, N. C. Murmu, and P. Banerjee, Corros. Sci. 146 (2019) 134.
[3]   M. A. Hegazy, A. S. El-Tabei, A. H. Bedair, and M. A. Sadeq, RSC Adv. 5 (2015) 64633.
[4]   A. Ostovari, S. M. Hoseinieh, M. Peikari, S. R. Shadizadeh, and S. J. Hashemi, Corros. Sci. 51 (2009) 1935.
[5]   A. P. Yadav, F. Suzuki, A. Nishikata, and T. Tsuru, Electrochim. Acta 49 (2004) 2725.
[6]   M. Dahmani, A. Et-Touhami, S. S. Al-Deyab, B. Hammouti, and A. Bouyanzer, Int. J. Electrochem. Sci. 5 (2010) 1060.
[7]   P. Mourya, S. Banerjee, and M. M. Singh, Corros. Sci. 85 (2014) 352.
[8]   A.Y. El-Etre, Mater. Chem. Phys. 108 (2008) 278.
[9]   Y. Qiang, S. Zhang, B. Tan, and S. Chen, Corros. Sci. 133 (2018) 6.

[10] H. Cang, Z. Fei, J. Shao, W. Shi, and Q. Xu, Int. J. Electrochem. Sci. 8 (2013) 720.

[11] A.Y. El-Etre, J. Colloid Interface Sci. 314 (2007) 578.

[12] G. Choudhary, A. Sharma, R. K. Bangar, and A. Sharma, IJIRAE. 2 (2015) 112.

[13] N. Soltani, N. Tavakkoli, M. K. Kashani, and A. Mosavizadeh, Journal of Industrial and Engineering Chemistry 20 (2014) 3217.

[14] P. S. Desai, Eur. J. Pharm. Med. Res. 2 (2015) 470.

[15] N. A. Odewunmi, S. A. Umoren, Z. M. Gasem, S. A. Ganiyu, and Q. Muhammad, J. Taiwan Inst. Chem. Eng. 51 (2015) 177.

[16] S. A. Umoren, I. B. Obot, A. U. Israel, P. O. Asuquo, M. M. Solomon, U. M. Eduok, and A. P. Udoh, J. Ind. Eng. Chem. 20 (2014) 3612.

[17] N. A. Odewunmi, S. A. Umoren, and Z. M. Gasem, J. Environ. Chem. Eng. 3 (2015) 286.

[18] A. S. Fouda, G. Y. Elewady, D. Shalabi, and S. Habouba, Int. J. Innov. Res. Sci. Eng. Technol. 3 (2014) 11210.

[19] P. Muthukrishnan, B. Jeyaprabha, and P. Prakash, Int. J. Ind. Chem. 5 (2014) 1.

[20] A. Hamdy, and N. S. El-Gendy, Egypt. J. Pet. 22 (2013) 17.

[21] L. Bammou, M. Belkhaouda, R. Salghi, O. Benali, A. Zarrouk, H. Zarrok, and B. Hammouti, J. Assoc. Arab Univ. Basic Appl. Sci. 16 (2014) 83.

[22] A. A. Khadom, A. N. Abd, and N. Arif, South Afr. J. Chem. Eng. 25 (2018) 13.

[23] N. I. Kairi, and J. Kassim, Int. J. Electrochem. Sci. 8 (2013) 7138.

[24] S. B. Ulaeto, U. J. Ekpe, M. A. Chidiebere, and E. E. Oguzie, Int. J. Mater. Chem. 2 (2012) 158.

[25] A. Singh, V. K. Singh, and M. A. Quraishi, Int. J. Corr. 2010 (2010)

[26] R. Karthik, P. Muthukrishnan, A. Elangovan, and B. Jeyaprabha, Adv. Civil Eng. Mater. 3 (2014) 413.

[27] A. Aytac, U. Ozmen, and M. Kabasakaloglu, Mater. Chem. Phys. 89 (2005) 176.

[28] P. R. Shrestha, H. B. Oli, B. Thapa, Y. Chaudhary, D. K. Gupta, A. K. Das, K. B. Nakarmi, S. Singh, N. Karki, and A. P. Yadav, Eng. J. 23 (2019) 205.

[29] B. Thapa, D. K. Gupta, and A. P. Yadav, J. Nepal Chem. Soc. 40 (2019) 25.

[30] N. Karki, Y. Chaudhary, and A. P. Yadav, J. Nepal Chem. Soc. 39 (2018) 76.

[31] P. C. Lama, Y. Chaudhary, N. Karki, and A. P. Yadav, J. Nepal Chem. Soc. 34 (2016) 120.

[32] R. Lama, A. K. Das, B. Yadav, Y. Chaudhary, P. C. Lama, S. L. Shrestha, D. K. Gupta, N. Karki, and A. P. Yadav, J. Nepal Chem. Soc. 38 (2018) 48.

[33] Y. Chaudhary, N. Karki, and A. P. Yadav, J. Nepal Chem Soc. 35 (2016) 139.

[34] Y. Li, P. Zhao, Q. Liang, and B. Hou, Appl. Surf. Sci. 252 (2005) 1245.

[35] L. Na, G. Hui, Z. Peng, Z. Xin, Z. Lihua, and A. Singh, Int. J. Electrochem. Sci. 14 (2019) 1830.

[36] N. Karki.,S. Neupane, Y. Choudhary, U. Singh, and A. P. Yadav, Surf. Interfaces. (2020). https://www.journals.elsevier.com/surfaces-and-interfaces, in press.

[37] R. Thusa, and S. Mulmi, Nepal J. Biotechnol. 5 (2017) 5.

[38] V. Chander, J. S. Aswal, R. Dobhal, and D. P. Uniyal, The Journal of Phytopharmacology 6 (2017) 53.

[39] P. Taylor, V. Bajpai, A. Singh, K. R. Arya, M. Srivastava, and B. Kumar, Food Additives & Contaminants: Part A 32 (2015) 37.

[40] W. Li, X. Zhao, F. Liu, and B. Hou, Corros. Sci. 50 (2008) 3261.

[41] C. B. Verma, and M. A. Quraishi, Electrochem. Surface Anal. 3 (2014) 14601.

[42] F. Bentiss, M. Bouanis, B. Mernari, M. Traisnel, H. Vezin, and M. Lagrene, Applied Surface Sci. 253 (2007) 3696.

[43] V. Sivakumar, K. Velumani, and S. Rameshkumar, Mate. Res. 21 (2018) 1.

[44] R. Sadeghi, M. Amirnasr, S. Meghdadi, and M. Talebian, Corros. Sci. 151 (2019) 190.